Comparative numerical analysis of various geometric configurations of a two-dimensional heat sink.

Djellid Ikram [1], Bouhamri Noureddine [2], Bouhafs Mohamed [3], Boualem Ikram [4], Bouzit Fayçel [5]

[1,2,3,4] *Lab of Industrial Production and Maintenance Engineering, Institute of Maintenance and Industrial Safety, University of Oran2 Mohamed Ben Ahmed; P.B 1015 El M'naouer 31000 Oran Algeria*

E-mail : djellid.ikram@univ-oran2.dz, noured_bh@yahoo.fr, mohamedbouhafs@yahoo.fr, boualem.ikram.31@gmail.com.

[5]*Lab of Maritime Sciences and Engineering LSIM Faculty of Mechanical Engineering, University of Science and Technology of Oran, Mohamed Boudiaf, El M'naouer, B.P.1505, 31000, Oran, Algeria*

E-mail : faycal.bouzit@yahoo.fr.

Abstract: Comparative numerical analysis of the thermal and hydraulic performance of a turbulent flow of incompressible air through a heat sink plat pin-fin (PPFHS) of circular and semi-circular, with and without baffles. The K-ε model was used for numerical calculations of the geometric configuration of this 2D heat sink to see the influence of geometry on heat dissipation with a change in velocity from 6.5 m/s to 12.2 m/s. The results show a 51% improvement in thermal resistance of the semi-circular PPFHS with baffles compared with the circular PPFHS.

Keywords: heat sink, thermal resistance, turbulent flow, PPFHS, geometry.

1. INTRODUCTION

Researchers have carried out a great deal of research to improve the performance of heat sinks, with the aim of increasing the performance of electronic systems. Electronic components need to be adequately cooled to avoid overheating and to ensure a longer service life.

In engineering technology, it is becoming increasingly important to achieve efficient cooling of electronic systems. Engineers are pursuing new heat sink designs as a means to cope with the rising demands. (Da Silva et al., 2019) conducted a comprehensive analysis of natural convection in heat sinks with rectangular fins using numerical simulations and experimental tests. They investigated factors influencing heat transfer in such devices, developed empirical correlations for the convective heat transfer coefficient. Microchannel heat sinks with pin ribs and fins have also been investigated (Ghasemi et al., 2017). Computational simulations of plate fin, strip fin, and pin fin heat sinks revealed the influence of flow rates on their performance (Li et al., 2023).

Plate-pin fin heat sinks had different pin shapes that influenced convection(Jonsson & Moshfegh, 2001). Ranging from turbulent to laminar flows induced by arrays of square-shaped blocks were examined (Zhou & Catton, 2011). Nanofluids composed of MWCNTs-CuO-Water have been tested in microchannel flow cells at various concentrations in order to increase their thermal dissipation effects (Bouchenafa et al., 2015). The study by Yu et al (2005). compared the thermal performance of a plate-fin heat sink and a pin-fin heat sink and showed a 30% reduction in thermal resistance for the pin-fin heat sink. The geometric dimensions of the heat sink and flow conditions were necessary to evaluate the heat transfer efficiency.

Recent studies have also explored natural convection from rectangular interrupted fins (Ahmadi et al., 2014), highlighting the influence of fin interruptions on heat dissipation performance.

These studies illustrate how engineers are trying to make both devices cooler and more efficient by redesigning better heat sinks.

In this work, a comparative numerical analysis of the thermal and hydraulic performance of a turbulent flow of incompressible air through a rectangular channel-shaped heat sink, interspersed with circular and semi-circular fins, with or without baffles in the upper and lower inner wall, was carried out. To see the effect of geometry on heat dissipation as the air entry velocity changes 6.5, 8, 10, 12.2 (m/s). This work was carried out after validating the simulations by comparing them with experimental (Yu et al., 2005) and Numerical results (Zhou & Catton, 2011).

2. PROBLEM DESCRIPTION

2.1 geometric configuration of the problem

Figure 1.a.b.c.d. shows the geometry considered in this work. The figures represent a rectangular channel of dimensions L and H containing three circular (a) and semi-circular (b) blocks. Figures (c) and (d) have the same dimensions as figures (a) and (b) with the addition of triangular baffles in the inner wall of the channel. Table 1 shows the dimensions of the four model studied.

Table 1. Dimension of geometry

L(mm)	H(mm)	x(mm)	y(mm)	w(mm)	z(mm)
51	5	13	3	8	5

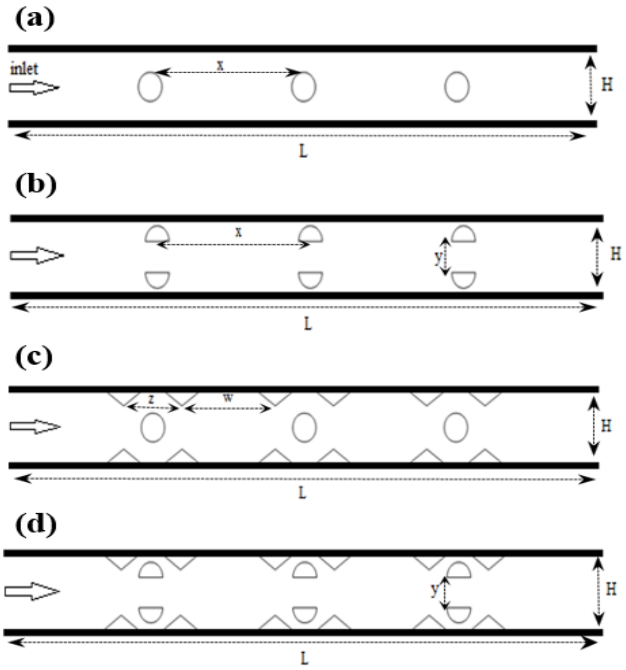

Figure 1. Geometry of the problem. a/ circular b/ semi-circular c/ circular with baffles d/ semi-circular with baffles.

2.2 Governing equation

The flow is assumed as Bidimensional problem, turbulent, incompressible, and steady flow, uniform velocity profile at the inlet, Physical properties of fluid (air) and solid are constant, and radiation is neglected.
The utilization of governing equations (continuity, momentum, and energy) is involved in simulating steady fluid flow that is incompressible and heat transfer. (Bouchenafa et al., 2015)

Continuity

$$\frac{\partial}{\partial x_i}(\rho u_i) = 0 \tag{1}$$

Momentum

$$\frac{\partial}{\partial x_j}(\rho u_i u_j) = -\frac{\partial P}{\partial x} + \frac{\partial}{\partial x_j}\left[\mu\left(\frac{\partial u_i}{\partial x_j} + \frac{\partial u_j}{\partial x_i}\right)\right] \tag{2}$$

Energy

$$\frac{\partial}{\partial x_i}(\rho u_i T) = \frac{\partial}{\partial x_j}\left(\Gamma \frac{\partial T}{\partial x_j}\right) \tag{3}$$

2.3 k-ε turbulent model

The k-epsilon (k-ε) turbulence model is based on two transport equations: one for the turbulent kinetic energy (k) and one for the turbulent kinetic energy dissipation rate (ε). These equations are formulated as follows:

$$\frac{\partial}{\partial x_j}(\rho \overline{u_j} k) = \frac{\partial}{\partial x_j}\left[\left(\mu + \frac{\mu_t}{\sigma_k}\right)\frac{\partial k}{\partial x_j}\right] + \mu_t\left(\frac{\partial \overline{u_i}}{\partial x_j} + \frac{\partial \overline{u_j}}{\partial x_i}\right).\frac{\partial \overline{u_i}}{\partial x_j} - \rho\varepsilon \tag{4}$$

$$\frac{\partial}{\partial x_j}(\rho \overline{u_j} \varepsilon) = \frac{\partial}{\partial x_j}\left[\left(\mu + \frac{\mu_t}{\sigma_\varepsilon}\right)\frac{\partial \varepsilon}{\partial x_j}\right] + C_1 \frac{\varepsilon}{k}\mu_t\left(\frac{\partial \overline{u_i}}{\partial x_j} + \frac{\partial \overline{u_j}}{\partial x_i}\right).\frac{\partial \overline{u_i}}{\partial x_j} - C_2\rho\frac{\varepsilon^2}{k} \tag{5}$$

For the k-e model, the constant terms are presented in Table 2.

Table 2. Constants of k–ε model

constant	C_μ	C_1	C_2	σ_k	σ_ε
value	0.09	1.44	1.92	1.0	1.3

Where μ_t is the turbulent viscosity, for flows with high Reynolds numbers can be represented by (Yu et al., 2005)

$$\mu_t = \rho C_\mu \frac{k^2}{\varepsilon} \tag{6}$$

2.4 Boundary conditions

The boundary conditions applied to solve the aforementioned governing equations in the current computations are

- The Inlet

$$u = u_{in}, \qquad v = 0, \qquad T = T_{in} \tag{7}$$

- The Outlet

$$\frac{\partial \emptyset}{\partial x} = 0, \qquad \emptyset = u, v, k, T, \varepsilon. \tag{8}$$

- The Walls of cannel

$$u = v = 0, \qquad \frac{\partial T}{\partial x} = 0 \tag{9}$$

- Solid blocks

$$T = T_w \tag{10}$$

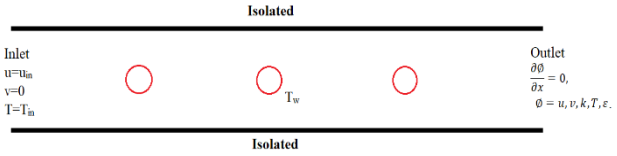

Figure 2. Boundary conditions.

3. NUMERICAL RESOLUTION

In this work, the COMSOL Multiphysics programme, which is based on the finite element method, was used to realise the numerical simulation.

3.1 Validation of results

Validation of the calculation model and the numerical simulation method was carried out via a study using calculation software. This simulation was validated by comparing its results with experimental data from (Yu et al., 2005)and (Zhou & Catton, 2011). In figure 3, we see the variation in pressure drop plotted as a function of inlet velocities; this result confirms the accuracy of our approach as it aligns well with both sets of existing data. Good agreement between these results means that this issue can be examined numerically.

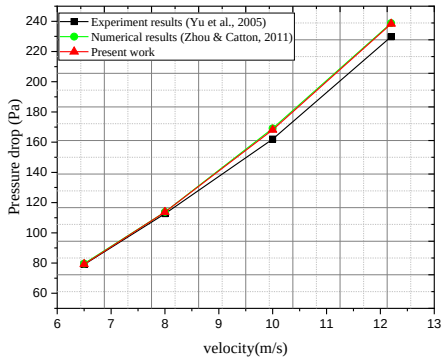

Figure 3. Comparison of our pressure drop results with those of experimental and numerical studies.

4. RESULTS AND DISCUSSION

To investigate the effect of block spacing and addition of baffles on heat transfer and flow performance for different heated blocks located inside the channel, numerical simulations were conducted under 10 W heat flux and variable inlet velocities of 6.5, 8, 10 and 12.2 m/s. The results are presented as thermal resistance and spatial representation of velocity at inlet velocity of 10 m/s.

4.1 Distribution of flow fields

From the velocity profiles shown in figures 4, 5, 6 and 7 where the inlet velocity is 10 m/s .It can be seen that recirculation zones are formed behind the blocks and between the baffles near the inner walls due to the separation of air by the latter. The size of the recirculation zones is larger in the case of a circular than a semi-circular fin and smaller in the case of adding baffles.

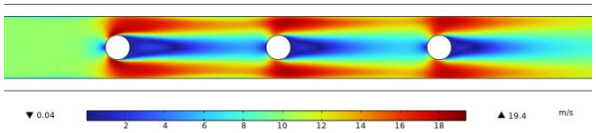

Figure 4. Spatial representation of velocity for the PPFHS circular (u_{in}=10m/s).

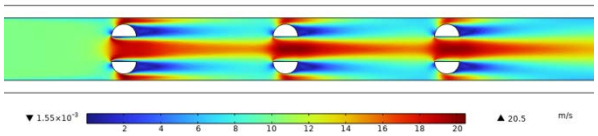

Figure 5. Spatial representation of velocity for the PPFHS semi-circular (u_{in}=10m/s).

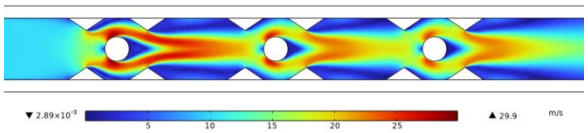

Figure 6. Spatial representation of velocity for the PPFHS circular with baffles (u_{in}=10m/s).

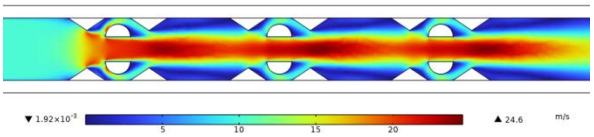

Figure 7. Spatial representation of velocity for the PPFHS semi-circular with baffles (u_{in}=10m/s).

4.2 Thermal resistance

The thermal resistance of the heat sink, R_{th}, can be defined by. (Yu et al., 2005)

$$R_{th} = \frac{\Delta T}{Q} \qquad (11)$$

Where ΔT is the difference between the average temperature at the bottom and the air temperature (T). Q is the heat rate.

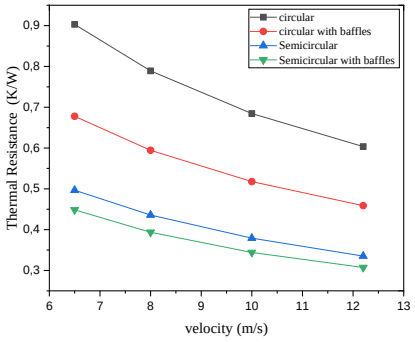

Figure 8. Thermal resistance as a function of velocity for different geometries.

The thermal resistance for the different studied cases of the heat sink for different inlet velocities in figure 8 is obtained using equation (11). The figure shows that the thermal resistance of the heat sink decreases with increasing inlet velocity in all cases, and the thermal resistance of the semicircular fin heat sink with baffles is about 51% lower than the thermal resistance of the circular fin heat sink.

5. CONCLUSION

The study, which involved conducting a numerical analysis to examine the effect of design and geometry on the thermal behaviour of a two-dimensional heat sink in the form of a rectangular channel with heated blocks of different geometries, proved that dividing the heated blocks increases the contact area between them and the cooled fluid and thus significantly reduces the thermal resistance.

The addition of baffles allows the liquid flow to be directed, increasing the velocity and the contact area between the fluid and the heated blocks, thereby significantly improving convection. The reduction in thermal resistance was estimated to be 51% when the blocks were split and baffles were added, compared to circular blocks without baffles. This demonstrates the effectiveness of this model in optimising heat transfer.

REFERENCES

Ahmadi, M., Mostafavi, G., & Bahrami, M. (2014). Natural convection from rectangular interrupted fins. *International Journal of Thermal Sciences*, *82*, 62-71. https://doi.org/10.1016/j.ijthermalsci.2014.03.016

Bouchenafa, R., Saim, R., & Abboudi, S. (2015). Numerical study of forced convection in a turbulent heat sink made of several rows of blocks of square form. *Heat and Mass Transfer*, *51*(9), 1301-1311. https://doi.org/10.1007/s00231-015-1496-4

Da Silva, V. A., De Neves Gomes, L. A. C., De Lima E Silva, A. L. F., & De Lima E Silva, S. M. M. (2019). Analysis of natural convection in heat sink using OpenFOAM and experimental tests. *Heat and Mass Transfer*, *55*(8), 2289-2304. https://doi.org/10.1007/s00231-019-02574-5

Ghasemi, S. E., Ranjbar, A. A., & Hosseini, M. J. (2017). Numerical study on effect of CuO-water nanofluid on cooling performance of two different cross-sectional heat sinks. *Advanced Powder Technology*, *28*(6), 1495-1504. https://doi.org/10.1016/j.apt.2017.03.019

Jonsson, H., & Moshfegh, B. (2001). Modeling of the Thermal and Hydraulic Performance of Plate Fin, Strip Fin, and Pin Fin Heat Sinks—Influence of Flow Bypass. *IEEE TRANSACTIONS ON COMPONENTS AND PACKAGING TECHNOLOGIES*, *24*(2).

Li, C., Li, X., Huang, H., & Zheng, Y. (2023). Hydrothermal performance analysis of microchannel heat sink with embedded module with ribs and pin-fins. *Applied Thermal Engineering*, *225*, 120167. https://doi.org/10.1016/j.applthermaleng.2023.120167

Yu, X., Feng, J., Feng, Q., & Wang, Q. (2005). Development of a plate-pin fin heat sink and its performance comparisons with a plate fin heat sink. *Applied Thermal Engineering*, *25*(2), 173-182. https://doi.org/10.1016/j.applthermaleng.2004.06.016

Zhou, F., & Catton, I. (2011). Numerical Evaluation of Flow and Heat Transfer in Plate-Pin Fin Heat Sinks with Various Pin Cross-Sections. *Numerical Heat Transfer, Part A: Applications*, *60*(2), 107-128. https://doi.org/10.1080/10407782.2011.588574